OPEN ACCESS

Original research

Relationship between impaired BMP signalling and clinical risk factors at early-stage vascular injury in the preterm infant

Motaharehsadat Heydarian ®,[1] Prajakta Oak,[1] Xin Zhang,[1] Nona Kamgari,[1] Alida Kindt,[2] Markus Koschlig,[1] Tina Pritzke,[1] Erika Gonzalez-Rodriguez,[1] Kai Förster ®,[1,3] Rory E Morty,[4] Friederike Häfner,[1] Christoph Hübener,[5] Andreas W Flemmer,[3] Ali Oender Yildirim ®,[1] Deepti Sudheendra,[6] Xuefei Tian,[6] Agnese Petrera,[7] Holger Kirsten,[8] Peter Ahnert,[8] Nick Morrell,[9] Tushar J Desai,[6] Jennifer Sucre,[10] Edda Spiekerkoetter,[6] Anne Hilgendorff[1,11]

Linked

► http://dx.doi.org/10.1136/thorax-2022-219482

Check for updates

ABSTRACT

Introduction Chronic lung disease, that is, bronchopulmonary dysplasia (BPD) is the most common complication in preterm infants and develops as a consequence of the misguided formation of the gas-exchange area undergoing prenatal and postnatal injury. Subsequent vascular disease and its progression into pulmonary arterial hypertension critically determines long-term outcome in the BPD infant but lacks identification of early, disease-defining changes.

Methods We link impaired bone morphogenetic protein (BMP) signalling to the earliest onset of vascular pathology in the human preterm lung and delineate the specific effects of the most prevalent prenatal and postnatal clinical risk factors for lung injury mimicking clinically relevant conditions in a multilayered animal model using wild-type and transgenic neonatal mice.

Results We demonstrate (1) the significant reduction in BMP receptor 2 (BMPR2) expression at the onset of vascular pathology in the lung of preterm infants, later mirrored by reduced plasma BMP protein levels in infants with developing BPD, (2) the rapid impairment (and persistent change) of BMPR2 signalling on postnatal exposure to hyperoxia and mechanical ventilation, aggravated by prenatal cigarette smoke in a preclinical mouse model and (3) a link to defective alveolar septation and matrix remodelling through platelet derived growth factor-receptor alpha deficiency. In a treatment approach, we partially reversed vascular pathology by BMPR2-targeted treatment with FK506 in vitro and in vivo.

Conclusion We identified impaired BMP signalling as a hallmark of early vascular disease in the injured neonatal lung while outlining its promising potential as a future biomarker or therapeutic target in this growing, high-risk patient population.

KEY MESSAGES

WHAT IS ALREADY KNOWN ON THIS TOPIC

⇒ Bone morphogenetic protein receptor 2 (BMPR2) signalling is a hallmark of pulmonary arterial hypertension.

WHAT THIS STUDY ADDS

⇒ Impaired BMPR2 signalling characterises vascular pathology at its earliest stage in the injured neonatal lung and can thus be considered a potential driver, treatable target and biomarker of disrupted pulmonary development in preterm infants with chronic lung disease, that is, bronchopulmonary dysplasia.

HOW THIS STUDY MIGHT AFFECT RESEARCH, PRACTICE AND/OR POLICY

⇒ Our study demonstrates a comprehensive approach including human data and a preclinical, multilayered experimental model meticulously unravelled clinically relevant details of altered BMPR2 signalling in the developing lung undergoing prenatal and postnatal injury, thereby linking vascular pathology during alveolar septation to this critical modulator of pulmonary vessel disease.

INTRODUCTION

Chronic lung disease (CLD), that is, bronchopulmonary dysplasia (BPD) affects more than 30% of all preterm infants and is characterised by the impaired formation of the gas-exchange area as a result of prenatal and postnatal injury perturbing physiological alveolar and vascular development.[1]

Following the rarefication of the vascular bed that is tightly intertwined with alveolar simplification[2] the development of pulmonary vascular disease (PVD) and the risk for subsequent pulmonary arterial hypertension (PAH) is one of the most severe complications in infants with BPD.[3 4] Despite the undeniable clinical significance, earliest, yet disease relevant hallmarks characterising and driving the onset of PVD and later contributing to the progression into PAH, are poorly understood in the BPD context.

In adults and children, critical mechanisms leading to the development of PAH converge on bone morphogenetic protein receptor 2 (BMPR2) signalling[5 6] with re-establishment of functional BMPR2 signalling representing a key therapeutic goal.[7–9] Despite the compelling clinical evidence for the significance of the pathway in PVD[10 11] as well as in organogenesis[12 13] the role of BMPR2 in early stage vascular pathology and its relation to the most prevalent clinical risk factors that provoke chronic disease in the preterm lung (CLD) has not been comprehensively explored.[14]

We; therefore, investigated changes in BMPR2 expression in preterm infants with BPD by visualising RNA transcription in the diseased lung, correlating plasma proteomics in BPD infants with structural changes in lung MRI and addressing heritable traits of altered BMP signalling in BPD by the means of a genetic association study in n=1000 preterm infants. We assessed the dynamics of BMPR2 signalling as a developmentally relevant, established driver of vascular disease in response to the most prevalent prenatal and postnatal risk factors for adverse lung development using a multilayered neonatal mouse model. In this model, exposure to clinically relevant levels of mechanical ventilation (MV) and hyperoxia (O_2) as pivotal postnatal risk factors[15] was next combined with the prenatal impact of non-growth restricting doses of cigarette smoke (CS), known to affect one third of all pregnancies.[16–18] We aimed to anchor BMPR2 signalling in the context of impaired alveolarisation by the use of platelet derived growth factor receptor alpha (PDGF-Rα) deficient mice, thereby addressing the interconnection of both pathways and the link of BMPR2 expression levels to alveolar septation and matrix formation.[19 20] Finally, we investigated therapeutic strategies using FDA-approved drugs applied in PAH[9] to reverse vascular pathology in the injured neonatal lung in vitro and in vivo.

RESULTS

BMP protein expression as an indicator of early lung vascular injury in preterm infants developing BPD

Physiologically, pulmonary endothelial BMPR2 expression is increased in the developing lung of a preterm when compared with a term infant (figure 1A). In disease, we demonstrated an early decrease in BMPR2 expression in CD31 positive cells in the lung periphery of preterm infants postnatally exposed to MV in comparison to age-matched infants who died in the first hours of life (figure 1B). Partial correlation networks of $\log_2$ transformed protein expression profiles obtained from proteome analysis (day of life 28+; figure 1C) revealed a negative correlation between proteins of the BMPR2 and PDGF signalling cascade and signs of emphysema and interstitial remodelling as obtained by MRI. The network accounted for BPD, days of MV, days of O_2 supplementation and GA (blue line: negative correlation, orange line: positive correlation; octagons: proteins, rectangles: clinical variables; edges significant at false discovery rates (FDR)<0.25). Assessing the impact of hereditary traits on the postnatal impairment in BMPR2 signalling, we performed genetic association analysis for 26 BMPR2-related genes in 1061 preterm infants (n=278 cases with moderate/severe BPD) considering case control status and length of oxygen and/or MV exposure. In 1016 single-nucleotide polymorphisms (SNP) out of 5632 SNPs with nominal significance (p≤0.05), classical BMPR2 polymorphisms known for their relevance in PAH were not associated with the presence of BPD or the duration of MV or oxygen exposure when accounting for multiple testing (online supplemental figure S1). One SNP (rs72917751-C), located in

the *SMAD7* gene in a genomic region and predicted to be relevant for increased gene transcription in several human tissues including the lung, was associated with the duration of oxygen supplementation (p=1.7×10^{-5}, FDR=0.48; figure 1D).

Impaired BMP signalling in the developing lung in an early stage of PVD resulting from exposure to the most prevalent risk factors for lung injury in the preterm infant

In our preclinical neonatal mouse model (figure 2A), we showed that O_2 and MV for only 8-hour provoke a significant reduction in pulmonary BMPR2 signalling as reflected by the three-fold reduction in lung protein levels of pSMAD 1-5-9 and its downstream target ID-1 (figure 2B). These changes occur during the earliest stage of lung vascular injury in a critical phase of alveolarisation (postnatal day (PND) 5–8), accompanied by a twofold induction of endothelial cells (EC) apoptosis and a reduction in micro vessel number (20–100 µm diameter; figure 2C). Pulmonary expression of the hypoxia inducible factor (HIF) 1α in these mice remained unchanged (online supplemental figure S2A).

A causal relationship between impaired BMPR2 and EC signalling in the neonatal lung is demonstrated by the use of BMPR2 heterozygote mice, exhibiting decreased baseline levels of lung VE-Cadherin expression and its subsequent reduction on postnatal O_2 exposure (figure 2D). Indicating prolonged effects of MV and O_2 on BMPR2 expression levels, we (1) confirmed the downregulation of BMPR2 expression after extended periods of MV (24 hours) by the use of IHC in vivo (figure 2E) and (2) validated these findings in vitro by imaging RNA expression levels in neonatal mouse precision cut lung slices (PCLS) showing a decrease in BMPR2 transcription in VE-Cadherin positive cells on oxygen exposure for 24 hours (figure 2F). Long-term effects of the early impairment in BMPR2 signalling are demonstrated in 18 months old animals, where lung BMPR2 signalling remained significantly decreased after only 8 hours of moderate postnatal O_2 at PND 5, complying effects obtained with higher O_2 levels (FiO$_2$=0.85) (online supplemental figure S2B).

Prenatal exposure to CS resulting in increased pulmonary vulnerability to postnatal injury and aggravated impairment of BMP signalling

In order to assess the additional impact of prenatal lung injury on BMP signalling in the context of early postnatal vascular pathology, we exposed pregnant mice to non-growth-restricting doses of CS, one of the most prevalent prenatal toxins (figure 3A, online supplemental figure S3A). Proving prenatal effects of CS on the developing lung, we demonstrated increased protein levels for pulmonary cytochrome P450 1A1 (CYP1A1) and decreased levels for pulmonary secreted protein acidic and rich in cysteine (SPARC) in the lungs of these neonatal mice (PND 5–8) in comparison to filtered air (FA) controls (online supplemental figure S3B,C). Prenatal CS resulted in increased pulmonary vulnerability towards postnatal lung injury induced by O_2 and MV-O_2 exposure with early-stage vascular injury being tied to a significant reduction in BMP signalling, that is, decreased expression of SMAD 1-5-9 and ID1 as well as BMP4 in total lung homogenates (figure 3B). Pulmonary inflammation as a characteristic sign of lung injury was indicated by accumulation of lung monocytes/macrophages and increased TGF-β signalling following pCS exposure (figure 3C,D). These changes led to increased apoptosis (online supplemental figure S3D) with a twofold increase of VE-Cadherin and cleaved-caspase-3 double positive cells and a subsequent decrease in EC and micro vessel number
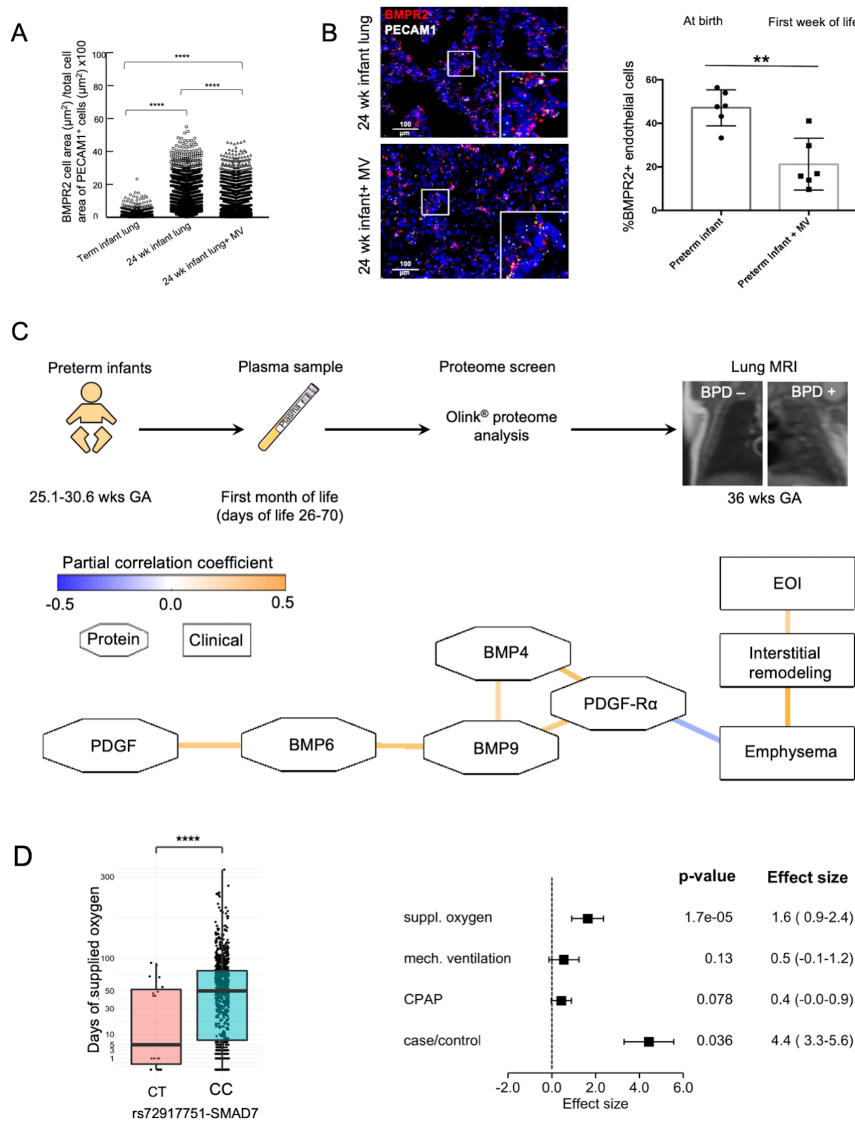
Figure 1 Decrease in lung vasculature BMPR2 expression and reduced BMP and PDGF plasma levels in preterm infants with BPD in the absence of relevant genetic variants. ISH quantification of BMPR2 and PECAM1 +double positive cells (positive cell area/total cell area; $\mu m^2/\mu m^2$) showed (A) the physiological increase in BMPR2 expression per endothelial cell in the developing preterm lung when compared with a term newborn as well as the decrease with mechanical ventilation (MV) in a preterm infant at the same age, that is, 24 weeks gestational age (GA) and (B) a significant reduction of overall pulmonary microvascular BMPR2 expression in the preterm infant undergoing postnatal lung injury induced by the exposure to MV for 2–8 weeks (24–26 weeks GA at birth; n=3/group) when compared with age-matched infants who died in the first days of life . (C) EDTA plasma samples were obtained in preterm neonates GA 25.1–30.6 weeks) with (1) and without (0) BPD at days of life 26–70 and subjected to proteome analysis (Olink proteomics). Infants were characterised for their lung structural changes at term by lung MRI (T2-weighted single-shot fast-spin-echo (ssFSE) sequences;) MRI left panel: infant without BPD, MRI right panel: infant with severe BPD in coronal plane showing interstitial enhancement and emphysematous changes. The partial correlation network of log_2 transformed protein expression profile obtained by proteome analysis (day of life 28+) reveals a negative correlation between the protein levels of the BMPR2 and PDGF-Rα signalling cascade and the development of emphysema and interstitial remodelling. The network accounts for BPD, days of MV, days of O_2 supplementation and GA (blue line: negative correlation, orange line: positive correlation; octagons: proteins, rectangles: clinical variables). All edges are significant at false discovery rate (FDR)<0.25. (D) Association of rs72917751-*SMAD7* with time of supplemented O_2. Rounded gene doses for the rs72917751 genotypes (imputed). association analysis was done using area sinus hyperbolicus transformed values of the time of supplemented oxygen (p=1.7×10^{-5}, FDR=0.48). Association was adjusted for relatedness, gender, gestational age, birth weight <10 th percentile, and country of maternal origin. Effect size of rs72917751-*SMAD7* in human genetic association analysis. Association of rs72917751 was investigated with BPD case–control status and three measures of respiratory support (area sinus hyperbolicus transformed). Phenotypes were adjusted for relatedness, gender, gestational age, birth weight <10 th percentile and country of maternal origin. Data are mean±SD **p<0.01, ****p<0.0001. BMPR2, bone morphogenetic protein receptor 2; BPD, bronchopulmonary dysplasia; ISH, RNA in situ hybridization.

(figure 3E,F; online supplemental figure S3E). Vascular pathology was further characterised by structural remodelling of the lung vessels indicated by the increased presence and adverse distribution of mature elastic fibres in the vessel wall

(online supplemental figure S4A). These changes occurred in the context of alveolar simplification and were mirrored by the overall increase in smooth muscle actin (SMA) expression in the lung periphery (online supplemental figure S4B).
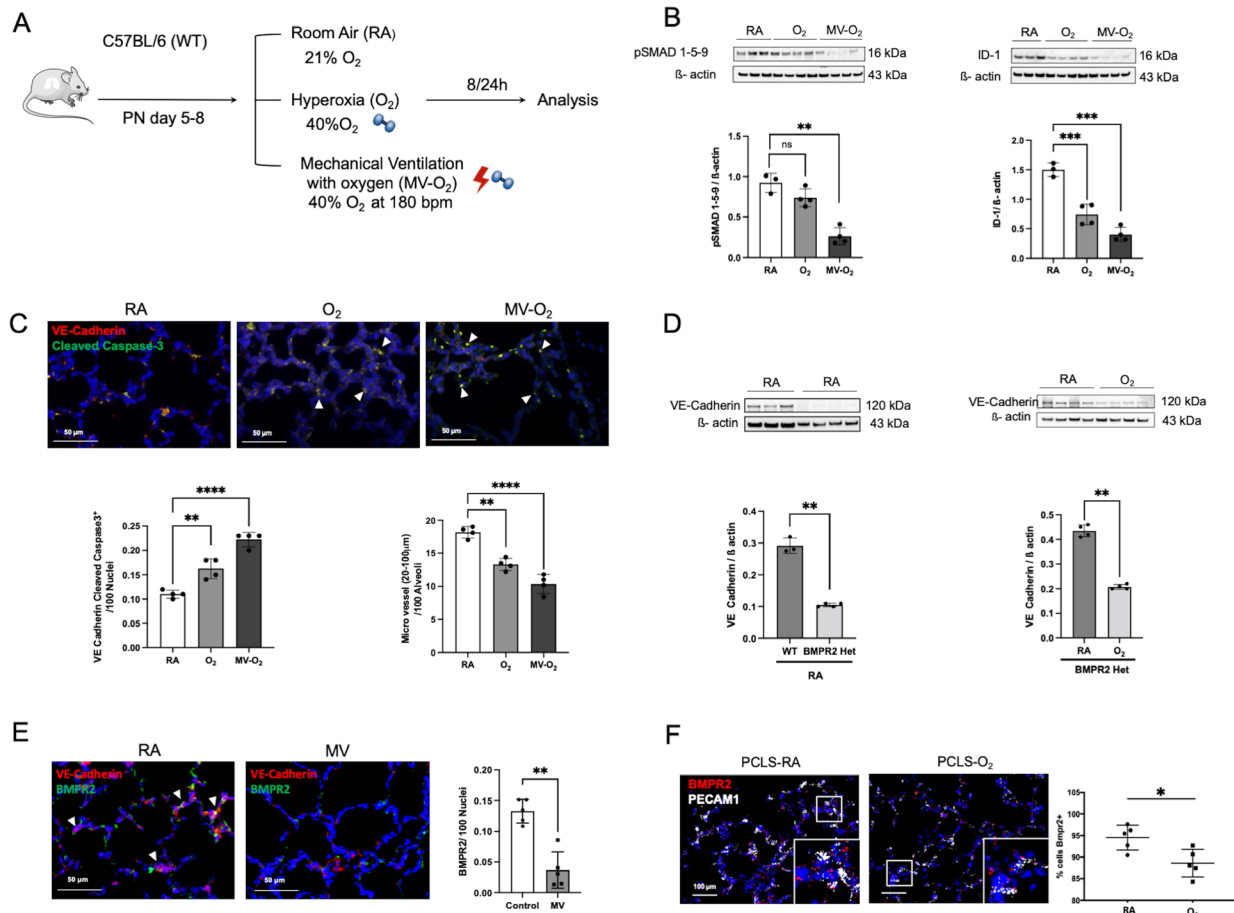
Figure 2 Significant reduction in BMP signalling at the earliest stage of lung vascular pathology is accompanied by microvessel loss in postnatal lung injury. (A) Preclinical mouse model of bronchopulmonary dysplasia (BPD) with induction of lung injury by exposure of neonatal mice to mechanical ventilation (MV) and/or hyperoxia (FiO_2=0.4) for 8 hours or 24 hours. (B) Immunoblot analysis reveals a significant decrease in pSMAD 1-5-9 and Id-1 protein levels in WT mice in the early course of postnatal lung injury provoked by short-term MV-O_2 and O_2 exposure. (C) Representative images of immunofluorescence (IF) staining for cleaved caspase-3 (green) and VE-cadherin positive cells (red) in lung tissue sections (4 µM, 400X, upper panel; nuclei (DAPI, blue) from 5 to 8 day old pups show a significant increase in EC apoptosis, confirmed by quantitative analysis (lower-left panel). Histological analysis reveals a significant decrease in the number of micro vessels (20–100 µm diameter) in the lungs of mice undergoing only 8 hours of O_2 and/or MV when compared with room air (RA) controls (lower-right panel). (D) In BMPR2 deficient mice, immunoblot analysis demonstrates significantly lower VE-cadherin protein expression in the neonatal lung at baseline (RA) when compared with WT pups (left panel). Postnatal exposure to moderate O_2 further decreases VE-cadherin protein expression in BMPR2 deficient mice (right panel). (E) Representative images of immunofluorescence (IF) staining for BMPR2 (green) and VE-cadherin positive cells (red) in lung tissue sections (4 µM, 400X, upper panel; nuclei (DAPI, blue) following 24 hours MV show a prolonged and significant decrease in BMPR2 expression, confirmed by quantitative analysis (right panel). (F) ISH demonstrates a persistent decrease in BMPR2 transcription in neonatal mouse PCLS exposed to O_2 for 24 hours when compared with RA control samples. Data are mean±SD *p<0.05, **p<0.01, ***p<0.001, ****p<0.0001, n=3–4 mice/group compared with RA controls. Quantification of if in 10 fields of view (FOV) per section in two sections per animal, normalisation of positive cells to 100 nuclei; arrows point to positive cells. ISH quantification in 212.55 µm x 212.55 µm FOV. BMP, bone morphogenetic protein; BMPR2, BMP receptor 2; ISH, RNA in situ hybridization; PCLS, precision cut lung slices; VE, vascular endothelial; WT, wild type.

Impaired BMP signalling linked to PDGF-dependent alveolar pathology in the neonatal lung

Linking impaired BMPR2 signalling to the onset of defective alveolar septation, we used transgenic newborn mice to study the impact of deficient PDGF-Rα signalling on BMPR2 function in the neonatal lung undergoing prenatal and postnatal injury (figure 4A). The decrease in PDGF-Rα, a consequence of myofi-broblast apoptosis during lung injury, resulted in the enhanced loss of septal quantity associated with structural abnormalities exceeding effects observed in WT littermates (figure 4B–D). These changes were accompanied by the aggravation of EC apoptosis and in the presence of impaired PDGF-Rα signalling, in line with a significant decrease in BMPR2 signalling, that is,

ID1 and pSMAD 1-5-9 expression, even exceeding the significant changes provoked by preatal and postnatal environmental hazards in WT littermates (figure 4E–G; online supplemental figure S5).

FK506 treatment restoring impaired BMPR2 signalling in vitro and in vivo

Confirming the in vivo effects, we demonstrated EC-specific effects of O_2 and stretch on human primary fetal pulmonary endothelial cells (HPMECs) in vitro (figure 5A): 24 hours exposure of HPMECs to moderate hyperoxia (FiO_2=0.4), mechanical stretch or the combination of both results in a significant
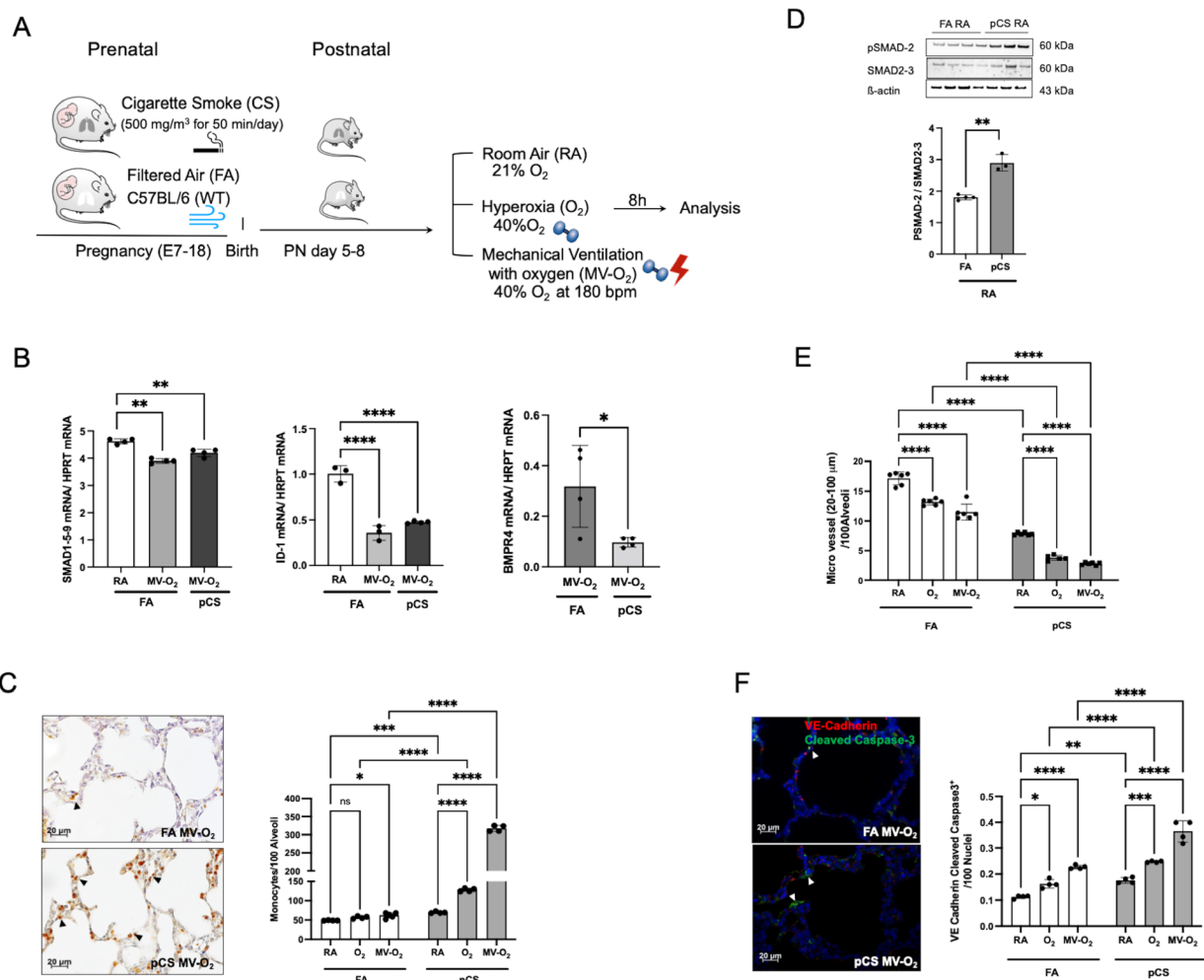
Figure 3 Early decrease in BMPR2 signalling in early lung vascular injury provoked by exposure to pCS. (A) In a preclinical BPD mouse model, neonatal mice were subjected to non-growth restricting doses of prenatal pCS followed by postnatal MV and/or O_2 (FiO$_2$=0.4). (B) Smad 1-5-9 (left panel) and ID1 (middle panel) mRNA expression show a comparable reduction after MV-O_2 exposure in pCS and FA mice, whereas BMP4 is further decreased in neonatal mice exposed to pCS followed by MV-O_2 as compared with FA controls (right panel). (C) Representative images of IHC stainings indicate increased presence of pulmonary monocytes/macrophages (F4/80) (4 µM, ×400, left panel) following pCS, aggravated by postnatal exposure to MV and/or O_2 (right panel), and resulting (D) in a significant increase of pulmonary TGF-ß activity, that is, lung pSMAD2 protein expression. (E) Histological analysis reveals a significant decrease in microvessel number (20–100 µm diameter) induced by pCS in the lungs of neonatal mice when compared with FA controls. (F) Representative images of if staining for cleaved caspase-3 (green) and VE-cadherin (4 µM, ×400, left panel; nuclei (DAPI, blue) in lungs of 5–8 days old pups show significantly enhanced lung EC apoptosis in pCS exposed pups, aggravated byMV and O_2 exposure (right panel). Data are mean±SD *p<0.05, **p<0.01, ***p<0.001, ****p<0.0001, n=3–6 mice/group. quantification of if images in 10 FOV per section in two sections per animal, normalisation of positive cells to 100 nuclei; arrows point to positive cells. ISH quantification in 212.55 µm x 212.55 µm FOV. BMPR2, bone morphogenetic protein receptor 2; BPD, bronchopulmonary dysplasia; EC, endothelial cell; FA, filtered air; FOV, fields of view; pCS, prenatal cigarette smoke.

downregulation of pSMAD 1-5-9 expression (figure 5B). When using mechanical stretch, this effect is enhanced by TGF-β (figure 5C) with maximum effects translating into reduced ID-1 protein levels (figure 5D) together with a decrease in SMAD 4 expression (figure 5E). To evaluate treatment strategies, we subsequently show the potential of FK506 (2 ng/mL) to ameliorate or reverse the effect of stretch and/or O_2 on BMPR2 signalling in HPMECs. A single dose of FK506 (2 ng/mL) results in increased pSMAD1-5-9 protein levels in HPMECs exposed to maximum injury, that is, O_2 and mechanical stretch with and without additional TGF-β (figure 5F). The effect of FK506 (2 ng/mL) on BMPR2 transcription in HPMECs exposed to O_2 (figure 5G) cannot be observed in human fetal fibroblasts, indicating its cell specificity (online supplemental figure S6A). A single intraperitoneal dose of 2 ng/mL FK506 increased

pulmonary CD31 transcription in vivo (figure 5H; online supplemental figure S6B) and restored VEGF-R2 protein expression (online supplemental figure S6C) in newborn mice in the earliest phase of postnatal injury, that is, exposure to MV-O_2 or O_2 (2 hours). In summary, impaired BMPR2 signalling can be highlighted as a hallmark of early-stage vascular disease in the neonatal lung undergoing prenatal and postnatal injury, aggravated in the context of decreased PDGF-Rα signalling and persisting long term (figure 6).

DISCUSSION

In this study, we demonstrated reduced pulmonary BMPR2 transcription and early postnatal reduction in related plasma protein levels in infants with characteristic lung structural changes. We addressed the
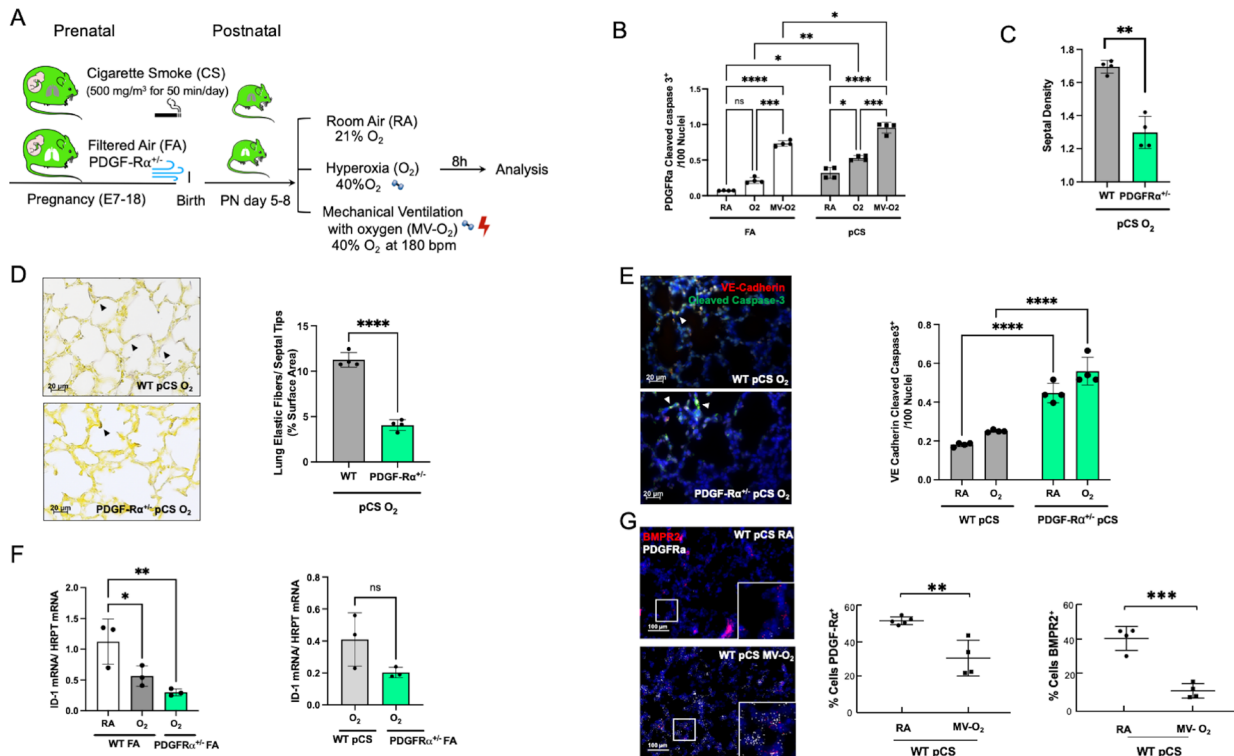
Figure 4 Aggravated loss of BMPR2 signalling and increased vascular pathology in the presence of BPD characteristic PDGF-Rα deficiency. (A) In our preclinical model, PDGF-Rα heterozygote (PDGF-Rα+/-) neonatal mice and WT littermates were exposed to pCS and postnatal MV and/or hyperoxia (FiO$_2$=0.4) for 8 hours. (B) Exposure to pCS resulted in a significant increase in apoptosis of PDGF-Rα expressing cells (PDGF-Rα and cleaved caspase-3 double positive cells), aggravated by postnatal exposure to O$_2$ or MV-O$_2$. (C, D). The reduction in PDGFR expression is accompanied by an increased loss of septal crests and elastic fibres (Hart's stain) on postnatal O$_2$ exposure (4 µM, 400X) in the lungs of 5–8 days old mice. (E) Quantification of if staining in lung tissue sections show enhanced EC apoptosis in PDGF-Rα$^{+/-}$ neonatal mice exposed to pCS and postnatal O$_2$, that is, increase in VE-cadherin (red) and cleaved caspase-3 (green) double positive cells (4 µM, ×400, left panel; nuclei (DAPI, blue). (F) Subsequently, mRNA analysis demonstrates decreased ID1 mRNA expression in lungs from PDGF-Rα$^{+/-}$ mice exposed to short-term postnatal O$_2$, exceeding the effect in WT littermates achieved by O$_2$ alone or in combination with pCS. (G) ISH quantification demonstrates the parallel decrease in PDGF-Rα and BMRPR2 transcription in WT mice undergoing prenatal and postnatal injury, that is, pCS and MV-O$_2$. Data are mean±SD. *P<0.05, **p<0.01, ***p<0.001, ****p<0.0001, n=3-4 mice/group. Quantitative analysis of IF images are performed in 10 fields of view (FOV) per section in a total of 2 sections per animal, normalisation of positive cells to 100 nuclei; arrows point to positive cells. ISH quantification in 212.55 µm x 212.55 µm. BMRPR2, bone morphogenetic protein receptor 2; BPD, bronchopulmonary dysplasia; EC, endothelial cell; FA, filtered air; MV, mechanical ventilation; PCS, prenatal cigarette smoke; WT, wild type.

impact of hereditary traits on early postnatal BMPR2 signalling in a genetic association study, and by the lack of an association suggest a role of secondary, environmental causes for the postnatal reduction in BMPR2 signalling in the preterm infant with evolving PVD.[21] In subsequent experimental studies that allowed us to assess the dynamics of BMPR2 signalling in a multilayered preclinical mouse model, we successfully demonstrated the significant reduction in BMPR2 expression in early PVD caused by both prenatal and postnatal injury. We thereby established impaired BMPR2 signalling, a hallmark of PAH together with early EC apoptosis and microvessel loss, as a result of the single or combined exposure to clinically relevant environmental insults, that is, moderate levels of MV and O$_2$[22 23] as well as non-growth restricting doses of CS.[18] The mimic of clinically relevant settings significantly added to previous studies using non-physiological injury conditions.[24]

As demonstrated in our study, the impairment of BMPR2 signalling occurs at the earliest stage of PVD during the critical window of alveolarisation, indicating its important role in BPD-related vascular pathology as opposed to a mere end-stage phenomenon. The loss of physiologically heightened BMP receptor and ligand expression levels likely results in lasting effects,[25] supported by our findings with a lack of compensatory upregulation in BMPR2 signalling after

short-term injury as well as its long-term impairment in adult mice following neonatal oxygen exposure. The decrease in BMPR2 signalling can be related to BPD characteristic inflammatory processes[26] in addition to the effects of oxygen[25] and mechanical shear stress[27 28] alone.

In line with previously published data from our group[19 29] differences in response to MV/stretch in combination with O$_2$ or O$_2$ alone can be observed in vitro and in vivo, suggesting the activation of both incremental as well as differential mechanisms.

Successfully anchoring impaired BMPR2 signalling in the context of BPD characteristic lung structural changes, we established its interdependency with PDGF-Rα expression, that is, known to hold critical functions in alveolar septation, extracellular matrix formation and vascular development.[19 20 30 31] The intertwined regulation of both pathways supports the relation of lung fibrosis and vascular pathology indicated by previous studies,[32 33] aggravated by the proliferation of apoptosis-resistant ECs in the presence of impaired BMPR2 signalling[34] and the subsequent exposure of subendothelial cells to growth factors and chemokines due to decreased EC barrier function.[35] Uncontrolled fibroblast proliferation likely increases further in the absence of higher-functioning PDGF-Rα positive fibroblast.[36] We recapitulated vascular remodelling showing the enhanced
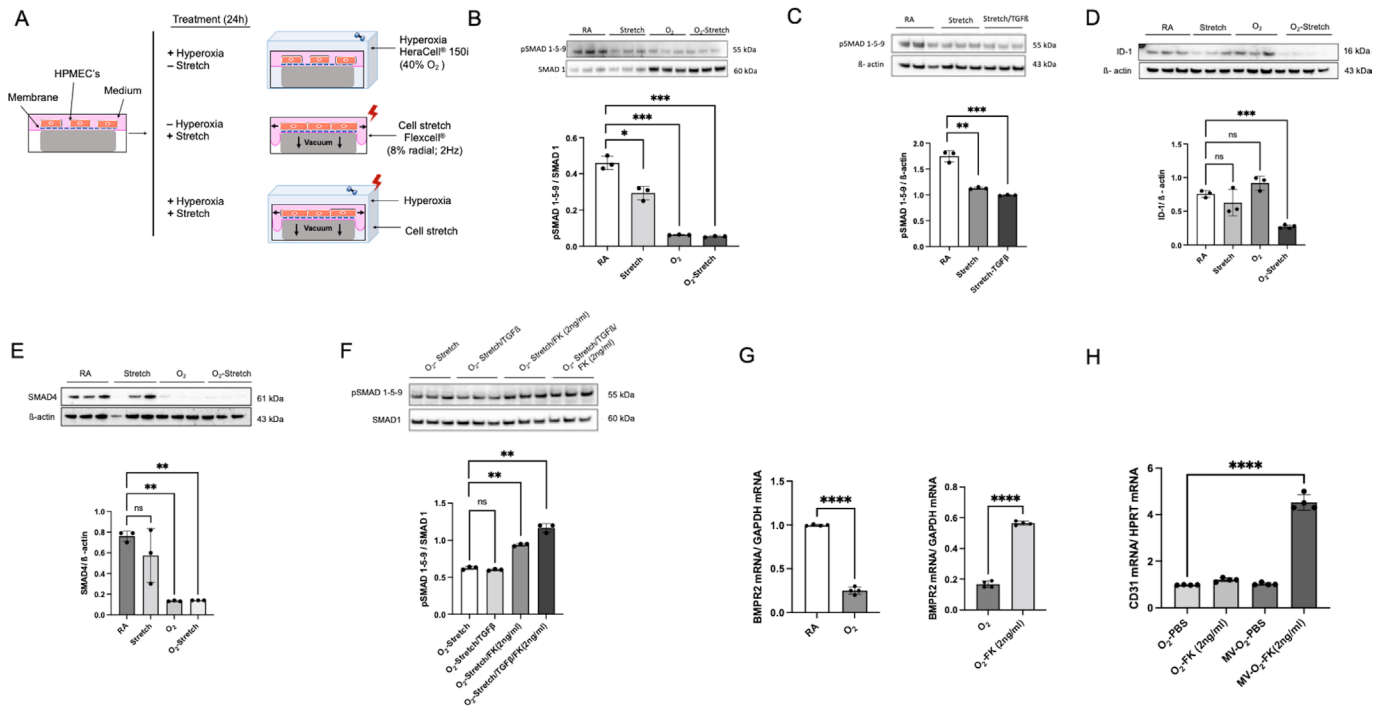
Figure 5 Impaired BMPR2 signalling is ameliorated on treatment with FK506 in vitro and in vivo. (A) Exposure of human pulmonary microvascular endothelial cells (HPMEC) to cyclic stretch or O_2 (FiO_2=0.4) for 24 hours in vitro mimics postnatal injury. (B) Immunoblot analysis shows a significant downregulation of pSMAD 1-5-9 protein expression in HPMECs after exposure to O_2 and/or stretch, (C) enhanced by TGF-β (D) and translated into decreased ID-1 and (E) Smad 4 protein expression. (F) Immunoblot analysis shows significant upregulation of pSMAD 1-5-9 protein levels in HPMECs on treatment with a single dose of 2 ng/mL FK506 in the presence of O_2 in combination with stretch and/or TGF-β incubation. (G) The significant reduction in BMPR2 mRNA levels after O_2 treatment is reversed by FK506 in HPMECs. (H) In vivo, a single intraperitoneal dose of 2 ng/mL FK506 in neonatal mice at the onset of O_2 or MV-O_2 exposure for 2 hours resulted in an upregulation of pulmonary CD31 mRNA expression levels in neonatal mice when compared with PBS treated control mice. Data are mean±SD *p<0.05, **p<0.01, ***p<0.001, ****p<0.0001, n=3–4 mice/group. BMPR2, bone morphogenetic protein receptor 2; ns, not significant; PBS, phosphate buffered saline.

presence of mature elastic fibres in the wall of small lung vessels side-by-side with alveolar simplification and interstitial remodelling after prenatal and postnatal lung injury.[19]

The observed relation of PDGF-Rα and BMPR2 signalling reflects impaired pathway cross-talk as demonstrated in mesenchymal cells,[37] with relevance for EC function[38] and VEGF-dependent EC survival,[19 39] underscoring the close relation of vascular and alveolar pathology.[2] Mimicking fibroblast loss through apoptosis, reduced PDGF-Rα expression negatively affects rescue mechanisms of BMP deficiency,[40] and BMP secretion by lung fibroblasts.[41] Studies demonstrated the decrease of ligand-activated endocytosis of the BMPR2 receptor in the presence of VEGF deficiency, thereby arresting its signalling.[42] Taken together with our findings, the lack of compensation for impaired BMPR2 signalling by, for example, HIF[2] or (PDGF-Rα dependent[19]) VEGF-A regulation hinders the restoration of EC signalling and vascular function in the neonatal lung, including abnormal metabolic and mitochondrial cell function.[25 26]

The potential of BMPR2 as a therapeutic target[5 6] is supported by the successful stimulation of BMPR2 signalling by the US Food and Drug Administration (FDA)-approved drug FK506 (Tacrolimus)[9] in a BPD-relevant context. In line with studies in adult PAH, FK506 rescued receptor expression and enhanced EC survival in vitro and in vivo during early injury. Although previous studies were unsuccessful to prevent BPD development by nitric oxide (NO) supplementation,[43] future studies in BPD should address the potency of prostacyclins, sildenafil, recombinant BMP9 or Elafin.[7–9 44 45] to restore impaired BMP signalling in the BPD lung while considering the coregulation of BMPR2 signalling with endothelin, NO[46] and surfactant production.[47]

In summary, we established impaired BMPR2 signalling in the early phase of PVD in response to the most prevalent clinical risk factors for lung injury and BPD development in preterm infants, thereby linking a hallmark of PAH with significant diagnostic and therapeutic potential to this high-risk patient cohort. The powerful combination of the most prevalent and relevant prenatal and postnatal risk factors for neonatal lung injury in a unique, multilayered preclinical animal model using wild-type and transgenic mice, enabled us to demonstrate both the dynamics as well as the clinical significance of reduced BMPR2 signalling hand-in-hand with the impaired expression of the respective signalling molecules in the circulation of the preterm infant with BPD. Aggravation of the BMP phenotype in the presence of impaired PDGF signalling points towards an important interaction of the pathways in BPD while reflecting on the interconnection of fibrosis development and vascular pathology. Testing the potential of the therapeutic stimulation of BMPR2 signalling in the injured neonatal lung, our study indicated the clinical potential of the BMP pathway as an indicator and therapeutic target of PVD in BPD.

Limitations of the study are the number of infants recruited for the translational studies, although we deem the number reasonable given the background of extreme prematurity. The lack of functional immaturity in the newborn mouse lung in comparison to the preterm infant requires additional preclinical studies to develop sufficient treatment options.

Following up on the results obtained by us, treatment strategies for preterm infant should be assessed for their potential to enhance BMP signalling, especially when aiming to improve vascular function and reduce risk for PVD. Future studies need to furthermore address the effect of reduced BMPR2 signalling in different cellular
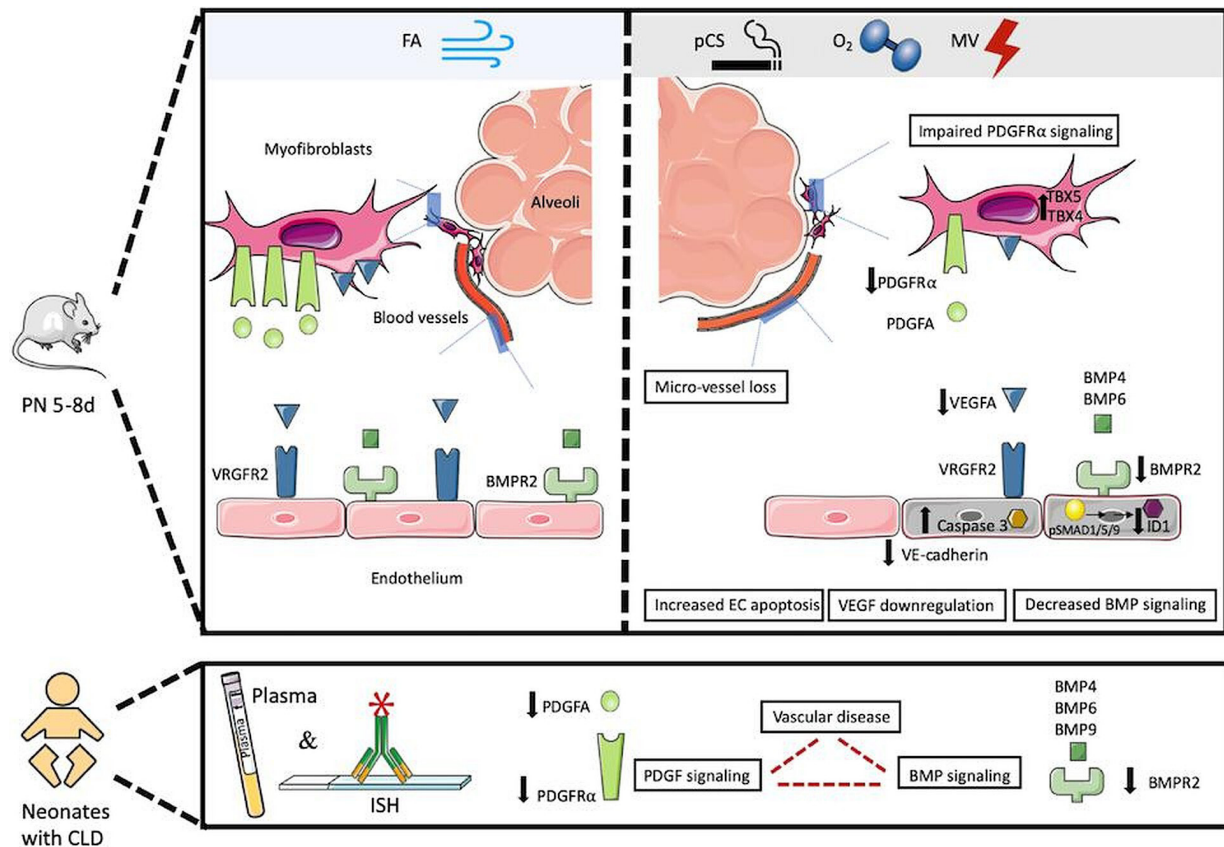
Figure 6 Graphical abstract. Impaired BMPR2 signalling as a hallmark of early-stage vascular disease in the neonatal lung undergoing prenatal and postnatal injury, aggravated in the context of decreased PDGF-Rα signalling and persisting long term. We demonstrate that the exposure of the preterm lung to postnatal injury provokes an early and significant decrease in endothelial BMPR2 expression, mirrored by the joined reduction of BMP and PDGF plasma protein levels in preterm infants with a developing chronic pulmonary condition. Using multilayered preclinical models, we delineate the specific effects of the most prevalent prenatal and postnatal clinical risk factors and show early endothelial cell apoptosis and microvessel loss tied to a significant decrease in BMP signalling. The changes in BMP signalling persist long-term, are causally related to impaired PDGF-Rα expression driving septation defects and can be targeted therapeutically using an FDA approved drug. in part, the schematic was created using Servier medical art templates, creative commons Attribution V.3.0 Unported license; https://smart.servier.com. BMP, bronchopulmonary dysplasia; BMPR2; BMP receptor 2; CLD, chronic lung disease; FA, filtered air; FDA, US Food and Drug Administration; MV, mechanical ventilation; pCS, prenatal cigarette smoke.

compartments of the neonatal lung, thereby providing insight into the interconnection of pathways in PVD and PAH development.

MATERIALS AND METHODS
Human studies
Human lung tissue analysis

Human lung tissue from autopsy specimens (EC #6 (Vanderbilt University) of preterm infants (23–26 weeks GA) that died within the first hours after birth or in the first week of life after MV and supplemental O2, respectively. Lung tissue from a term infant that died from a non-pulmonary cause served as a reference. sRNA in situ hybridisation by RNA scope (ACDBio) for BMPR2, PECAM1 (human), positive (Ppib) and negative (DapB) control was performed according to the manufacturer's instructions. Automated analysis by Halo software (Indica Labs) from fluorescent images used Keyence BZ-X710, BZ-X Viewer software (405, 488, 561, 647 nm; 400x). Comparative analysis was performed in two different ways: In figure 1A, each data point represents the result obtained for an individual cell quantifying the area of BMPR2 over total cell area (10 FOV/slide; 4 slides/infant). In figure 1B, each data point represents the overall %-positive BMPR2 cells in the lung periphery quantified in 10 FOV/slide, 4 slides/infant.[48]

Proteomic analysis in preterm plasma samples

Twenty-eight preterm infants <32 weeks GA with and without later development of BPD were included in the study (perinatal centre, LMU Hospital; EC #195-07). Plasma was derived from EDTA blood specimens at day of life 26–70. For patient characteristics, see online supplemental table S1. The infants have been characterised for lung structural changes (emphysema and interstitial remodelling) as assessed by MRI near term, that is, 36 weeks GA (3 Tesla MRI) using a 5-point Likert scale.

All samples (n=28) were randomised including inter-plate controls and measured by proximity extension assay (Olink Proteomics, Uppsala, Sweden: cardiometabolic (V.3602), cardiovascular II (V.5004), development (V.3511), inflammation (V.3012), metabolism (V.3402), neurology (V.8011), oncology II (V.7002)) following the manufacturer's instructions followed by quantification (Fluidigm BioMark HD Real-Time PCR). NPX values were intensity normalised (plate median for each assay as normalisation factor (Intensity Normalisation V.2); samples or proteins failing quality control were excluded. Partial correlation networks were calculated using R (V.4.0.0, package GeneNet (V1.2.15) with the ggm. estimate.pcor function after missing values were imputed using the imputeKNN method.[49]

Pulmonary MRI

Preterm infants underwent 3T MRI in spontaneous sleep at 36 weeks GA. T2-weighted single-shot fast-spin-echo sequences were quantified by a consensus panel of two senior neonatologists and two senior radiologists, blinded to the clinical diagnosis using defined criteria for scoring the presence of emphysema and interstitial enhancement on a 5-point Likert scale in four quadrants using coronal, axial and sagittal images.

Genetic association study

DNA extraction, genotyping and association analysis were performed as previously described.[50] Briefly, DNA was extracted from EDTA cord blood samples of n=1061 preterm infants (n=278 moderate/severe BPD[19]) ≤32 weeks GA. Clinical characteristics including days of invasive and non-invasive ventilation and O_2[51] were available for n=982 and 1029 infants and area sinus hyperbolicus transformed. Genotypes of patients were determined using Affymetrix Axiom microarrays (Axiom CEU array with custom content), imputation of the data used 1000 Genomes phase 1, V.3 as reference panel (genome built hg19/dbSNP 135). Association analysis of SNPs and case–control status as well as with history of respiratory support was adjusted for relatedness as previously described and accounted for gender, GA, birth weight <10th percentile and country of maternal origin. The role of genetic variants in the BMPR2 pathway used a total of 5632 SNPs (data.frame xl5, MAF filtering) with minor allele frequency ≥1% and imputed info score ≥0.5 in or near (±5 kb) the genes ACVR1, ACVR2A, ACVR2B, ACVRL1, BMP 2, BMP 4, BMP 6, BMP 7, BMPR1A, BMPR2, CAV1, Endoglin, FKBP1A, GDF2, ID1, SMAD1, SMAD2, SMAD3, SMAD4, SMAD5, SMAD7, SMAD9, TGFB1, TGFB2, TGFBR1 and TGFBR2. Correction for multiple testing was done using FDR (Benjamini and Hochberg).

Animal studies

Animal maintenance

For breeding, pathogen-free male and female C57BL/6 (wild-type, WT) and transgenic mice were obtained from Charles River (Sulzfeld, Germany) and housed at constant temperature and humidity, a 12-hour light cycle and food and water ad libitum. All animal experiments followed strict governmental and international guidelines approved by the local government for the administrative region of Upper Bavaria or by the Stanford University Institutional Animal Care and Use Committee.

Gene-targeted mice

PDGF-Rα haploinsufficient mice (B6.129S4-Pdgfra<tm11(EGFP)Sor/J>; no reported lung abnormalities) from Jackson laboratories (Bar Harbour, USA) were bred using heterozygous male and WT female mice to avoid effects of maternal PDGF-Rα heterozygosity. BMPR2 heterozygous mice (BMPR2$^{+/-}$; C57BL/6 background) were provided from Dr. Rabinovitch's Laboratory (Stanford University). Transgenic mice were compared with WT littermates.

pCS exposure

Pregnant female mice were exposed to whole-body active 100% mainstream total particulate matter (3R4F low tar modern research cigarettes (Tobacco Research Institute, University of Kentucky, USA), 500 mg/m³, 50 min, twice/day) from day 7 to 18 of gestation (total 10 days CS) using an exposure chamber via a membrane pump.[52] Controls received FA. After spontaneous delivery, pups were kept at RA with their mothers until postnatal day 5–8 (begin of experiments).

MV and O_2 experiments in neonatal mice

We randomly assigned term born 5–8-day-old male and female WT and transgenic mice (WT 3.7±0.5 g; body weight (bw), PDGF-Rα$^{+/-}$ 3.7±0.6 g; mean±SD) into three groups (13–16 mice per group), that is, 8h of MV with O_2 (MV-O_2, FiO_2=0.4,), O_2 only (FiO_2=0.4) and room air controls (FiO_2=0.21). As published previously.[19] mice underwent (1) tracheotomy after ketamine (≈60 µg/g bw) and xylazine (≈12 µg/g bw) sedation for MV-O_2 at 180 breaths/min (MicroVent 848; Harvard Apparatus, Holliston, MA; mimic of clinical conditions: mean tidal volume 8.68 µL/g bw; peak airway pressure 12-13cmH$_2$O, mean airway pressure 11-12cmH$_2$O) or (2) spontaneously breathed O_2 or RA after sham surgery under mild sedation.[19] Viable pups were euthanised (sodium pentobarbital) and lungs were harvested for analysis. For analysis of long-term effects, 5–8-day-old male and female WT mice were exposed to O_2 or RA with the mothers, kept alive, weaned using a standard procedure and sacrificed at 18 months of age. Sixteen 5–8-day-old WT newborn mice (3.7 g±0.5 g bw, mean±SD) received 2 ng/mL FK506 in 100 µL/g bw 0.9% sterile saline intraperitoneally or sterile saline only before the onset of MV-O_2.

Postmortem processing of lungs for quantitative histology

Lungs for histology from randomly selected mice (n=3/group) were fixed intratracheally with buffered 4%-PFA overnight @ 20 cmH$_2$O.[19] After paraffin-embedding and isotropic uniform random sectioning relative amount and distribution of insoluble lung elastin were obtained from Hart's elastin stain as previously described.[19] Representative pictures (3/animal) were obtained at 400x to assess alveolar and vascular structure.

Immunohistochemistry

Sections from 3 to 6 animals/group were incubated with peroxidase blocking reagent (Sigma, #31642), normal goat serum, primary antibodies (rat anti-F4/80; 1:400 ab6640 (Abcam)) and biotinylated goat anti-rat secondary antibody (1:200, Santa Cruz Biotechnology). Visualisation with streptavidin-HRP and diaminobenzidine (Dako, North America) was completed by counterstaining (haematoxylin (Richard-Allan Scientific, Kalamazoo, MI)) and mounting (Dako, North America, #S3023). Positively stained cells were quantified in 20 FOV/animal (400X magnification).

Immunofluorescence

Sections from (2–6 animals/group underwent antigen retrieval (0.1 M citric buffer, pH 6,≥96°C), tissue permeabilisation (Triton X-100 (0.5%), 20') and H$_2$O$_2$ treatment followed by antibody incubation (4°C overnight; PDGF-Rα (C-20, Santa Cruz Biotechnology #338), VE-Cadherin (H-72, Santa Cruz Biotechnology, #28644), cleaved caspase-3 (Cell Signalling Technology, #9661). Detection with Alexa 488/568 labelled goat anti-mouse antibody (Molecular Probes; Eugene, OR; 60') was complemented by DAPI counterstain (Sigma Aldrich #D8417). Total nuclei and single/double positive cells were quantified in 8 FOV/slide per animal (n=2–6 mice/group) (400x; IMARIS Software, Zurich, Switzerland).

Quantitative real-time RT-PCR

Total RNA from lung tissue homogenate was isolated using the peqlab-Gold Total RNA-Kit (Peqlab, Erlangen, Germany, #12-6834-01) before cDNA synthesis (random hexamers, MuLV reverse transcriptase (Applied Biosystems, Germany)). mRNA expression of target and housekeeping gene (hypoxanthine-guanine phosphoribosyltransferase, HPRT-1) expression was determined by Platinum SYBR Green qPCR SuperMix (Applied Biosystems; StepOnePlus 96 well RTPCR System (Applied Biosystems, CA) and displayed as $2^{-\Delta CT}$ ($\Delta C_T = C_{T\ target} - C_{T\ reference}$) or as $2^{-\Delta\Delta CT}$ values ($\Delta\Delta C_T = \Delta C_{T\ treated} - \Delta C_{T\ control}$).

Protein extraction and immunoblot analysis

Protein was extracted from snap-frozen total lungs using high urea buffer (KPO_4, Urea, AppliChem) with halt protease inhibitor (Thermo Fisher Scientific, #1861280); protein concentration measurement used BCA, Pierce Scientific Rockford, USA, #23227). Immunoblotting on Bis-Tris or Tris-Acetate gels (Life Technologies, Germany, #NP0321BOX, #EA0375BOX) included detection of CYP1A1 (A-9, Santa Cruz Biotechnology #SC-393979), ID1 (Abcam #ab168256), SMAD2/3 (Cell Signalling Technologies #3102), pSMAD2 (Cell Signalling Technologies #3101), SMAD 1 (Cell Signalling Technology, #6944), pSMAD 1-5-9 (Cell Signalling Technology, #9511), SMAD4 (Santa Cruz Biotechnology, #7966), SPARC (D10F10, Cell Signalling Technologies #8725), VE-Cadherin (H-72, Santa Cruz Biotechnology #28644), VEGF-A (147, Santa Cruz Biotechnology #507), VEGFR2 (R and D system, #AF644) and and β-actin (Santa Cruz Biotechnology, #sc-81178) (secondary antibodies goat anti-rabbit IgG (Santa Cruz Biotechnology, #2301) or goat anti-mouse IgG-HRP (Santa Cruz Biotechnology, #sc-81178)). Image quantification used chemiluminescence (ChemiDoc XRS+; GE Healthcare, Buckinghamshire, UK #RPN2232) and densitometry (Image Lab Software, Bio Rad, Munich, Germany).

In vitro experiments

Human pulmonary microvascular endothelial cells (HPMECs)

HPMECs (ScienCell Research Laboratories, CA, #3000) were cultured in ECM (ScienCell Research Laboratories, #1001) in 75 mL falcon flasks to 80%–90% confluency and seeded on flexible-bottomed laminin-coated 6 well plates (FlexCell International Corporation, #BF-3001L) for stretching experiments with 24 hours resting before experiments.

In vitro stretch

Cultured HPMEC's underwent cyclic strain by vacuum pressure (shape/sine; elongation min 0%, max 8%; frequency 2 Hz; duty cycle 50%; cycles 43216) for 24 hours before incubation with TGF-ß (5 ng/mL) and/or FK506 (2 ng/mL).

In vitro hyperoxia

Cultured HPMEC's underwent hyperoxia ($FiO_2 = 0.4$, 5% CO_2, 95% humidity, 37°C) or normoxia ($FiO_2 = 0.21$) for 24 hours before incubation with TGF-ß (5 ng/mL) and/or FK506 (2 ng/mL).

Immunoblot analysis

After cell lysis with RIPA buffer and halt protease inhibitor cocktail (Thermo Fisher Scientific, #1860932), determination of protein concentration and immunoblot analysis followed the above protocol.

Precision cut lung slices

The 300 μm PCLS from 4 to 7-day-old mice were cultured in DMEM-F12 for 24 hours in O_2 ($FiO_2 = 0.7$) or RA ($FiO_2 = 0.21$) (5% CO_2, 37°C) before formalin fixation, paraffin embedding and sectioning.[53]

RNA scope

RNA in situ hybridisation was performed as described above using Vim, Pdgfra, BMPR2 (mouse), positive (Ppib) and negative (DapB) control (ACDBio).

Statistical analysis

Statistical analysis was performed using the Prism V.8 software package (GraphPad, San Diego, California, USA). Multiple testing used two-way analysis of variance with Bonferroni correction; comparisons of two groups/parameters used student's unpaired t-test with Welch's correction. Results are given as mean and SD, numbers of each experiment are presented in the figures legend).

Analysis of proteomic and genetic association data is described above in the respective method's section.

Author affiliations
[1]Institute for Lung Biology and Disease and Comprehensive Pneumology Center with the CPC-M bioArchive, Helmholtz Zentrum München, Member of the German Center for Lung Research (DZL), Munich, Germany
[2]Division of Analytical Biosciences, Leiden Academic Centre for Drug Research (LACDR), Leiden University, Leiden, The Netherlands
[3]Department of Neonatology, Dr. v. Hauner Children's Hospital, Ludwig-Maximilians University, LMU Hospital, Munich, Germany
[4]Department of Translational Pulmonology, University Hospital Heidelberg, Translational Lung Research Center campus of the German Center for Lung Research (DZL), Heidelberg, Germany
[5]Department of Obstetrics and Gynecology, Ludwig-Maximilians University, LMU Hospital, Munich, Germany
[6]Department of Medicine, Division of Pulmonary, Allergy and Critical Care Medicine, Stanford University, Stanford, California, USA
[7]Research Unit Protein Science and Metabolomics and Proteomics Core, Helmholtz Zentrum München - German Research Center for Environmental Health, Neuherberg, Germany
[8]Institute for Medical Informatics, Statistics, and Epidemiology (IMISE), associated partner of the German Center for Lung Research (DZL), University of Leipzig, Leipzig, Germany
[9]Department of Medicine, Addenbrooke's Hospital, University of Cambridge, Cambridge, UK
[10]Mildred Stahlman Division of Neonatology, Department of Pediatrics, Vanderbilt University, Nashville, Tennessee, USA
[11]Center for Comprehensive Developmental Care (CDeCLMU), Ludwig-Maximilians University, LMU Hospital, Munich, Germany

Twitter Ali Oender Yildirim @AlionderCPC

Competing interests None declared.

Patient consent for publication Not applicable.

Ethics approval This study involves human participants and was approved by human lung tissue analysis: Vanderbilt University Institutional Review BoardProteomic analysis in preterm plasma samples: Ethics committees the Ludwig Maximilian-University (Ethics approval #195-07).

Provenance and peer review Not commissioned; externally peer reviewed.

Data availability statement Data are available on reasonable request.

ORCID iDs
Motaharehsadat Heydarian http://orcid.org/0000-0003-4411-5371
Kai Förster http://orcid.org/0000-0002-4127-1400
Ali Oender Yildirim http://orcid.org/0000-0003-1969-480X

REFERENCES
1 Hilgendorff A, Reiss I, Ehrhardt H, *et al*. Chronic lung disease in the preterm infant. lessons learned from animal models. *Am J Respir Cell Mol Biol* 2014;50:233–45.
2 Compernolle V, Brusselmans K, Acker T, *et al*. Loss of HIF-2alpha and inhibition of VEGF impair fetal lung maturation, whereas treatment with VEGF prevents fatal respiratory distress in premature mice. *Nat Med* 2002;8:702–10.
3 Mourani PM, Abman SH. Pulmonary vascular disease in bronchopulmonary dysplasia. *Curr Opin Pediatr* 2013;25:329–37.
4 Berkelhamer SK, Mestan KK, Steinhorn RH. Pulmonary hypertension in bronchopulmonary dysplasia. *Semin Perinatol* 2013;37:124–31.
5 Garcia-Rivas G, Jerjes-Sánchez C, Rodriguez D, *et al*. A systematic review of genetic mutations in pulmonary arterial hypertension. *BMC Med Genet* 2017;18:82.
6 Orriols M, Gomez-Puerto MC, Ten Dijke P. Bmp type II receptor as a therapeutic target in pulmonary arterial hypertension. *Cell Mol Life Sci* 2017;74:2979–95.
7 Nickel NP, Spiekerkoetter E, Gu M, *et al*. Elafin reverses pulmonary hypertension via caveolin-1-dependent bone morphogenetic protein signaling. *Am J Respir Crit Care Med* 2015;191:1273–86.
8 Yang J, Li X, Al-Lamki RS, *et al*. Sildenafil potentiates bone morphogenetic protein signaling in pulmonary arterial smooth muscle cells and in experimental pulmonary hypertension. *Arterioscler Thromb Vasc Biol* 2013;33:34–42.
9 Spiekerkoetter E, Tian X, Cai J, *et al*. Fk506 activates BMPR2, rescues endothelial dysfunction, and reverses pulmonary hypertension. *J Clin Invest* 2013;123:3600–13.
10 Trembath RC, Thomson JR, Machado RD, *et al*. Clinical and molecular genetic features of pulmonary hypertension in patients with hereditary hemorrhagic telangiectasia. *N Engl J Med* 2001;345:325–34.
11 Lyle MA, Fenstad ER, McGoon MD, *et al*. Pulmonary hypertension in hereditary hemorrhagic telangiectasia. *Chest* 2016;149:362–71.
12 Weaver M, Yingling JM, Dunn NR, *et al*. Bmp signaling regulates proximal-distal differentiation of endoderm in mouse lung development. *Development* 1999;126:4005–15.
13 Alejandre-Alcázar MA, Shalamanov PD, Amarie OV, *et al*. Temporal and spatial regulation of bone morphogenetic protein signaling in late lung development. *Dev Dyn* 2007;236:2825–35.
14 Goumans M-J, Zwijsen A, Ten Dijke P, *et al*. Bone morphogenetic proteins in vascular homeostasis and disease. *Cold Spring Harb Perspect Biol* 2018;10:a031989.
15 Davidson LM, Berkelhamer SK. Bronchopulmonary dysplasia: chronic lung disease of infancy and long-term pulmonary outcomes. *J Clin Med* 2017;6:4.
16 Mercelina-Roumans PE, Breukers RB, Ubachs JM, *et al*. Hematological variables in cord blood of neonates of smoking and nonsmoking mothers. *J Clin Epidemiol* 1996;49:449–54.
17 Martinez FD. Maternal risk factors in asthma. *Ciba Found Symp* 1997;206:233–9.
18 Gilliland FD, Berhane K, McConnell R, *et al*. Maternal smoking during pregnancy, environmental tobacco smoke exposure and childhood lung function. *Thorax* 2000;55:271–6.
19 Oak P, Pritzke T, Thiel I, *et al*. Attenuated PDGF signaling drives alveolar and microvascular defects in neonatal chronic lung disease. *EMBO Mol Med* 2017;9:1504–20.
20 Sun T, Jayatilake D, Afink GB, *et al*. A human YAC transgene rescues craniofacial and neural tube development in PDGFRalpha knockout mice and uncovers a role for PDGFRalpha in prenatal lung growth. *Development* 2000;127:4519–29.
21 Wang H, St Julien KR, Stevenson DK, *et al*. A genome-wide association study (GWAS) for bronchopulmonary dysplasia. *Pediatrics* 2013;132:290–7.
22 Alejandre-Alcázar MA, Kwapiszewska G, Reiss I, *et al*. Hyperoxia modulates TGF-beta/BMP signaling in a mouse model of bronchopulmonary dysplasia. *Am J Physiol Lung Cell Mol Physiol* 2007;292:L537–49.
23 Jobe AH. Animal models, learning lessons to prevent and treat neonatal chronic lung disease. *Front Med* 2015;2:1–13.
24 Yee M, White RJ, Awad HA, *et al*. Neonatal hyperoxia causes pulmonary vascular disease and shortens life span in aging mice. *Am J Pathol* 2011;178:2601–10.
25 Diebold I, Hennigs JK, Miyagawa K, *et al*. Bmpr2 preserves mitochondrial function and DNA during reoxygenation to promote endothelial cell survival and reverse pulmonary hypertension. *Cell Metab* 2015;21:596–608.
26 Pickworth J, Rothman A, Iremonger J, *et al*. Differential IL-1 signaling induced by BMPR2 deficiency drives pulmonary vascular remodeling. *Pulm Circ* 2017;7:768–76.
27 Hiepen C, Mendez P-L, Knaus P. It takes two to tango: endothelial TGFβ/BMP signaling crosstalk with mechanobiology. *Cells* 2020;9. doi:10.3390/cells9091965. [Epub ahead of print: 26 08 2020].
28 Doryab A, Tas S, Taskin MB, *et al*. Evolution of bioengineered lung models: recent advances and challenges in tissue mimicry for studying the role of mechanical forces in cell biology. *Adv Funct Mater* 2019;29:1903114.
29 Hilgendorff A, Parai K, Ertsey R, *et al*. Inhibiting lung elastase activity enables lung growth in mechanically ventilated newborn mice. *Am J Respir Crit Care Med* 2011;184:537–46.
30 Liebeskind A, Srinivasan S, Kaetzel D, *et al*. Retinoic acid stimulates immature lung fibroblast growth via a PDGF-mediated autocrine mechanism. *Am J Physiol Lung Cell Mol Physiol* 2000;279:L81–90.
31 Lindahl P, Karlsson L, Hellström M, *et al*. Alveogenesis failure in PDGF-A-deficient mice is coupled to lack of distal spreading of alveolar smooth muscle cell progenitors during lung development. *Development* 1997;124:3943–53.
32 Colombat M, Mal H, Groussard O, *et al*. Pulmonary vascular lesions in end-stage idiopathic pulmonary fibrosis: histopathologic study on lung explant specimens and correlations with pulmonary hemodynamics. *Hum Pathol* 2007;38:60–5.
33 Cao Z, Ye T, Sun Y, *et al*. Targeting the vascular and perivascular niches as a regenerative therapy for lung and liver fibrosis. *Sci Transl Med* 2017;9:1–15.
34 Rabinovitch M, Rabinovitch M. Molecular pathogenesis of pulmonary arterial hypertension. *J Clin Invest* 2012;122:4306–13.
35 Johnson JA, Hemnes AR, Perrien DS, *et al*. Cytoskeletal defects in Bmpr2-associated pulmonary arterial hypertension. *Am J Physiol Lung Cell Mol Physiol* 2012;302:L474–84.
36 Popova AP, Bentley JK, Cui TX, *et al*. Reduced platelet-derived growth factor receptor expression is a primary feature of human bronchopulmonary dysplasia. *Am J Physiol Lung Cell Mol Physiol* 2014;307:L231–9.
37 Li A, Xia X, Yeh J. Pdgf-Aa promotes osteogenic differentiation and migration of mesenchymal stem cell by down-regulating PDGFRA and derepressing BMP-Smad1/5/8 signaling. *PLoS One* 2014;9:1–21.
38 Hu W, Zhang Y, Wang L, *et al*. Bone morphogenic protein 4-smad-induced upregulation of platelet-derived growth factor AA impairs endothelial function. *Arterioscler Thromb Vasc Biol* 2016;36:553–60.
39 Suzuki Y, Montagne K, Nishihara A, *et al*. Bmps promote proliferation and migration of endothelial cells via stimulation of VEGF-A/VEGFR2 and angiopoietin-1/Tie2 signalling. *J Biochem* 2008;143:199–206.
40 Tripurani SK, Cook RW, Eldin KW, *et al*. BMP-specific Smads function as novel repressors of PDGFA and modulate its expression in ovarian granulosa cells and tumors. *Oncogene* 2013;32:3877–85.
41 Jeffery TK, Upton PD, Trembath RC, *et al*. Bmp4 inhibits proliferation and promotes myocyte differentiation of lung fibroblasts via Smad1 and JNK pathways. *Am J Physiol Lung Cell Mol Physiol* 2005;288:L370–8.
42 Hwangbo C, Lee H-W, Kang H, *et al*. Modulation of endothelial bone morphogenetic protein receptor type 2 activity by vascular endothelial growth factor receptor 3 in pulmonary arterial hypertension. *Circulation* 2017;135:2288–98.
43 Mercier J-C, Hummler H, Durrmeyer X, *et al*. Inhaled nitric oxide for prevention of bronchopulmonary dysplasia in premature babies (EUNO): a randomised controlled trial. *Lancet* 2010;376:346–54.
44 Long L, Ormiston ML, Yang X, *et al*. Selective enhancement of endothelial BMPR-II with BMP9 reverses pulmonary arterial hypertension. *Nat Med* 2015;21:777–85.
45 Yang J, Li X, Al-Lamki RS, *et al*. Smad-Dependent and Smad-independent induction of Id1 by prostacyclin analogues inhibits proliferation of pulmonary artery smooth muscle cells in vitro and in vivo. *Circ Res* 2010;107:252–62.
46 Gangopahyay A, Oran M, Bauer EM, *et al*. Bone morphogenetic protein receptor II is a novel mediator of endothelial nitric-oxide synthase activation. *J Biol Chem* 2011;286:33134–40.
47 Luo Y, Chen H, Ren S, *et al*. Bmp signaling is essential in neonatal surfactant production during respiratory adaptation. *Am J Physiol Lung Cell Mol Physiol* 2016;311:L29–38.
48 Schuler BA, Habermann AC, Plosa EJ, *et al*. Age-determined expression of priming protease TMPRSS2 and localization of SARS-CoV-2 in lung epithelium. *J Clin Invest* 2021;131. doi:10.1172/JCI140766. [Epub ahead of print: 04 01 2021].
49 Do KT, Wahl S, Raffler J, *et al*. Characterization of missing values in untargeted MS-based metabolomics data and evaluation of missing data handling strategies. *Metabolomics* 2018;14:128.
50 Blume F, Kirsten H, Ahnert P, *et al*. Verification of immunology-related genetic associations in BPD supports ABCA3 and five other genes. *Pediatr Res* 2021:1–9.
51 Stichtenoth G, Demmert M, Bohnhorst B, *et al*. Major contributors to hospital mortality in very-low-birth-weight infants: data of the birth year 2010 cohort of the German neonatal network. *Klin Padiatr* 2012;224:276–81.
52 John-Schuster G, Günter S, Hager K, *et al*. Inflammaging increases susceptibility to cigarette smoke-induced COPD. *Oncotarget* 2016;7:30068–83.
53 Sucre JMS, Vickers KC, Benjamin JT, *et al*. Hyperoxia injury in the developing lung is mediated by mesenchymal expression of Wnt5a. *Am J Respir Crit Care Med* 2020;201:1249–62.